Mechanics Research Communications 47 (2013) 39–43

Contents lists available at SciVerse ScienceDirect

Mechanics Research Communications

journal homepage: www.elsevier.com/locate/mechrescom

Acoustic signature of different fracture modes in marble and cementitious materials under flexural load

D.G. Aggelis [a,b,*], A.C. Mpalaskas [b], T.E. Matikas [b]

[a] Department of Mechanics of Materials and Constructions, Free University of Brussels, Pleinlaan 2, 1050 Brussels, Belgium
[b] Department of Materials Science and Engineering, University of Ioannina, Ioannina 45110, Greece

ARTICLE INFO

Article history:
Received 14 September 2012
Received in revised form 5 November 2012
Available online xxx

Keywords:
Acoustic emission
Bending
Shear
Marble
Cement mortar

ABSTRACT

The present study deals with the examination of the acoustic emission signatures of distinct fracture modes. Tensile and mixed mode cracking is excited in specimens of marble and cement mortar and the acoustic emission behavior is monitored. Tensile cracking incidents show a preference to higher frequencies and shorter waveforms unlike shear events. The results imply that adequate analysis of simple AE features enables the characterization of the current fracture condition of the material and consequently predictions on the remaining safe service life for monolithic, as well as microstructured materials.

1. Introduction

Fracture of structural materials in most cases follows a sequence; tensile stresses induce initial micro-cracking and later shear phenomena dominate as damage is being accumulated (Ohtsu, 2010). Identification of the active damage mode may well provide real time information on the status of the structural integrity of the material and allow predictions on its useful life span. Acoustic emission (AE) is a method suitable for damage monitoring since it utilizes the transient elastic waves after any crack propagation event. AE enables monitoring of crack growth with sensors mounted on the material surface. These sensors record the response after each cracking incident and transform it into electrical voltage due to their piezoelectric nature (Shull, 2002). Several laboratory efforts have been published concerning characterization of the cracking mode (Aggelis, 2011; Ohno and Ohtsu, 2010; Aggelis et al., 2010), monitoring of other processes like healing (Van Tittelboom et al., 2012) and progression of damage (Aggelis et al., 2011, Yonezu et al., 2010). However, in most of the cases of fracture monitoring, tensile cracking came from the direct tensile stresses on the matrix material (e.g. lower surface of a concrete beam under bending) while shear phenomena developed not by shear stresses directly on the matrix but by phenomena like frictional pull-out of steel fibers (Aggelis, 2011), detachment of reinforcing bars (Ohno and Ohtsu, 2010) or delamination between successive plies (Aggelis et al., 2010). In this study the shear cracking due to shear stresses on the matrix is directly targeted and the AE activity is compared to reference tests of tensile fracture on specimens of the same type and size. Two kinds of structural materials are used, namely marble and cementitious mortar. The first is an example of monolithic material while the latter contains microstructure in the size of few mm due to the sand grains. The interphase between the cement matrix and the grains may well dictate the path of the crack despite the external stress field and therefore, the acoustic behavior between fracture of the two material systems (monolithic and microstructural) can be compared. The experiments are conducted on a three point bending set up. Bending produces a fracture due to pure tensile stresses on the bottom surface of the material. With a slight modification of the set up, fracture due to shear stresses was also examined, as will be discussed below. Two AE transducers were used at certain distances from the crack in order to monitor the same AE event on two positions and make additional conclusions on the signal distortion as it propagates through different types of materials (Aggelis et al., 2012; Sause et al., 2012). This is important since AE signals, being elastic waves, suffer distortion and amplitude reduction due to scattering and damping. If this is not taken into account it may well result in erroneous conclusions when sensor separation distances are long since the basic characteristics of the waveforms are considerably changed compared to the emitted signal.

AE transducers are piezoelectric, and therefore the amplitude, A of a recorded AE waveform is measured in Volts or dB. Indications

* Corresponding author at: Department of Mechanics of Materials and Constructions, Free University of Brussels, Pleinlaan 2, 1050 Brussels, Belgium. Tel.: +32 2 629 3541.
E-mail addresses: daggelis@vub.ac.be, aggelis_d@yahoo.com (D.G. Aggelis).

0093-6413/$ – see front matter © 2012 Elsevier Ltd. All rights reserved.
http://dx.doi.org/10.1016/j.mechrescom.2012.11.007

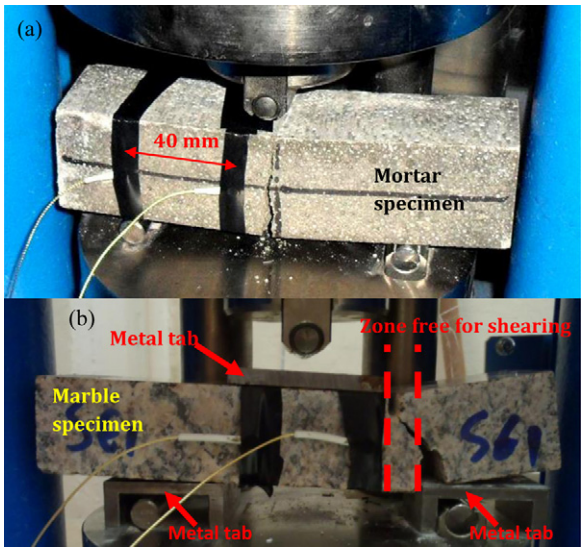

Fig. 1. (a) Three point bending test of mortar and (b) shear test of marble with concurrent AE monitoring by two sensors.

of the released – by the fracture event – energy are: the measured area under the rectified signal envelope, simply called "energy" or the "absolute energy" with units of Joule (Zárate et al., 2012). Other important parameters are the duration (delay between first and last threshold crossings), rise time, RT (delay between the first threshold crossing and peak amplitude point in μs) and RA, which is RT over A measured in μs/V. Representative frequency features are the average frequency, AF, which is the number of threshold crossings over the duration of a signal and the peak frequency, PF, which is the frequency of the spectrum with the maximum magnitude, both measured in kHz. It has been shown that RA undergoes a certain increase as the dominant fracture mode shifts from tensile to shear, while frequency indicators undergo strong decrease (Aggelis, 2011; Ohno and Ohtsu, 2010; Aggelis et al., 2010; Shiotani, 2006).

2. Experimental details

Two types of materials were used, namely cement mortar and marble. The specimens were prismatic of size 40 mm × 40 mm × 160 mm. Two similar mortar mixtures were produced consisting of six specimens each containing approximately 60 vol.% of sand grains the maximum size of which was 4.75 mm, while the water to cement ratio by mass was 0.55. This led to a density of 2217 kg/m^3. Six of the specimens were subjected to three-point bending according to EN 13892-2:2002, see Fig. 1a, with constant rate of loading. A slight modification was done for the other six specimens that were intended for study of the shear fracture mode. Specifically, a metal tab of length of 50 mm was placed on top center of the specimen (Fig. 1b). This was escorted by distributed support at the bottom considerably altering the stress field. While at the three point bending test, the crack is bound to start from the central point of the bottom side due to the tensile stresses, for the modified test, the metal tabs reduce the free bottom span and leave only a small zone available for shear fracture at one side of the specimen (right in Fig. 1b). The marble specimens were tested on the same experimental set up (three specimens for bending and three for shear). The specific slab used to cut the specimens was of the "Afyon white" marble type and had a density of 2727 kg/m^3. Fig. 1a and b shows typical specimens after the bending and shear test respectively.

Simple finite element stress analysis was also performed to evaluate the different stress fields for the "shear-like" experiment.

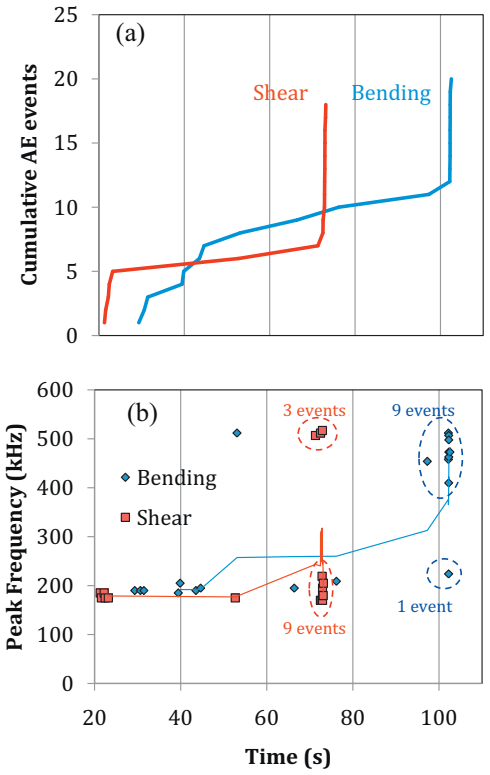

Fig. 2. (a) Cumulative events for bending and shear tests in two marble specimens. (b) Peak frequencies for the same events as recorded by the sensor at 15 mm away from the cracking zone. The symbols stand for the PF of the corresponding events, while the solid lines for the moving average of five points.

It was shown that at the unsupported zone (see Fig. 1b), the strongest stress component was shear although normal stresses were also developed. Therefore, it can be considered that pure tensile (from three point bending) and shear to mixed-mode fractures can be compared in this study. This analysis is not included in this manuscript due to the limited size of the manuscript.

AE measurements were conducted via two broadband sensors (Pico of Physical Acoustics Corporation, PAC). Their maximum sensitivity is at 450 kHz while their response from 300 to 600 kHz is within −3 dB from the maximum (see also PAC website). They were attached to the side of the specimen as seen in Fig. 1 with grease to enhance acoustic coupling, while they were secured by tape. The first sensor was placed in a horizontal distance of 15 mm from the cracking zone, while the second in 55 mm. The cracking position was secured by notches that were machined on marble specimens. The monitoring board was a two-channel PCI-2 of PAC and the sampling rate was 5 MHz. The threshold and the pre-amplifier gain were both set to 40 dB.

3. Results

Initially the behavior of representative specimens will be discussed and then the results will be generalized for the whole population of specimens. For both types of fracture tests, the acoustic emission cumulative activity exhibits a type of sigmoidal curve; a number of hits are recorded at an early stage of the experiment, followed by a period of moderate and constant emission rate, as seen in Fig. 2a for two marble specimens. The highest AE rate comes with the final fracture and the separation of the specimens in two parts. The cumulative number of events is approximately twenty for this kind of marble specimen. Concerning qualitative characteristics of AE, at the fracture moment of the shear experiment

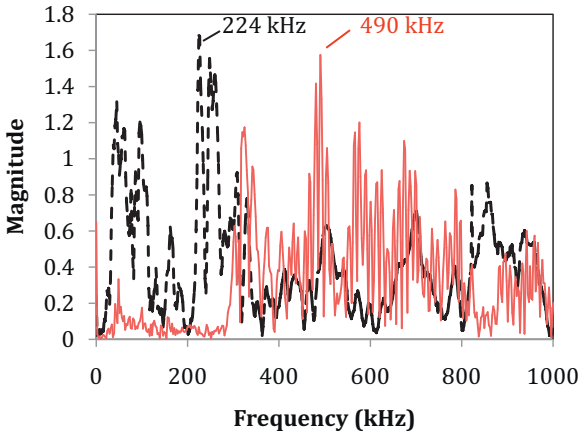

Fig. 3. FFT spectra of indicative AE waveforms of lower and higher peak frequencies.

(around 72 s), out of twelve recorded events, only three exhibited peak frequency (PF) around 500 kHz and nine PF around 200 kHz (see Fig. 2b). On the contrary for the bending experiment and the corresponding moment of macroscopic fracture just after 100 s, out of totally ten recorded events, only one exhibited frequency around 200 kHz and nine between 400 and 500 kHz. This observation shows that events due to pure tensile stresses show a preference to higher frequencies, while shear or mixed-mode show preference to lower ones. Representative FFT spectra from the two groups of the signals (of higher and lower peak frequency) are seen in Fig. 3. The first has a peak magnitude at 224 kHz (typical of shear) while the other at 490 kHz which is typical of tensile cracking in this study. Apart from the peak of 224 kHz, the "shear" spectrum exhibits content below 200 kHz while the "tensile" has negligible content below 300 kHz but exhibits random peaks up to 800 kHz.

This trend indicatively depicted for two specimens is generalized for the whole population of the AE events recorded during fracture of the bending and shear specimens. Fig. 4a shows the correlation plot between PF and rise time (RT) for all the events recorded by the nearest transducer (15 mm from the crack) for the whole population of marble specimens (three for shear and three for bending test). For shear fracture only a small portion of the population reaches 500 kHz, while most of the signals are below or around 200 kHz. For the signals coming from bending test the population is approximately equally dispersed in the bands of 100–200 kHz and 400–500 kHz, resulting in an average value of 300 kHz, considerably higher than the 242 kHz of shear, see large symbols in Fig. 4a. Fig. 4b shows the same events as captured by the furthest transducer (55 mm away from the crack). The results follow the same general trend while the frequencies are reduced due to the accumulated effect of attenuation of the longer distance. This decrease may seem limited, but considering that it occurs over just 40 mm of additional propagation between the two sensors, it bears great significance for larger specimens and definitely for actual application in structures, as will be discussed later.

The results of Fig. 4a and b concern marble material which can be considered macroscopically homogeneous. Similar experiments have been conducted in cementitious materials, as mentioned earlier. These specimens have microstructure in the form of sand grains, air bubble of similar size to the sand grains, as well as capillary porosity. In this case due to the weak cement paste – sand interphase the path of the crack is dictated around grains since they are stiffer than the matrix. Therefore, even though macroscopically a stress situation can be assumed or a stress field calculated, this may well differ from the actual stress condition responsible for the crack propagation around the microstructure. This was the reason

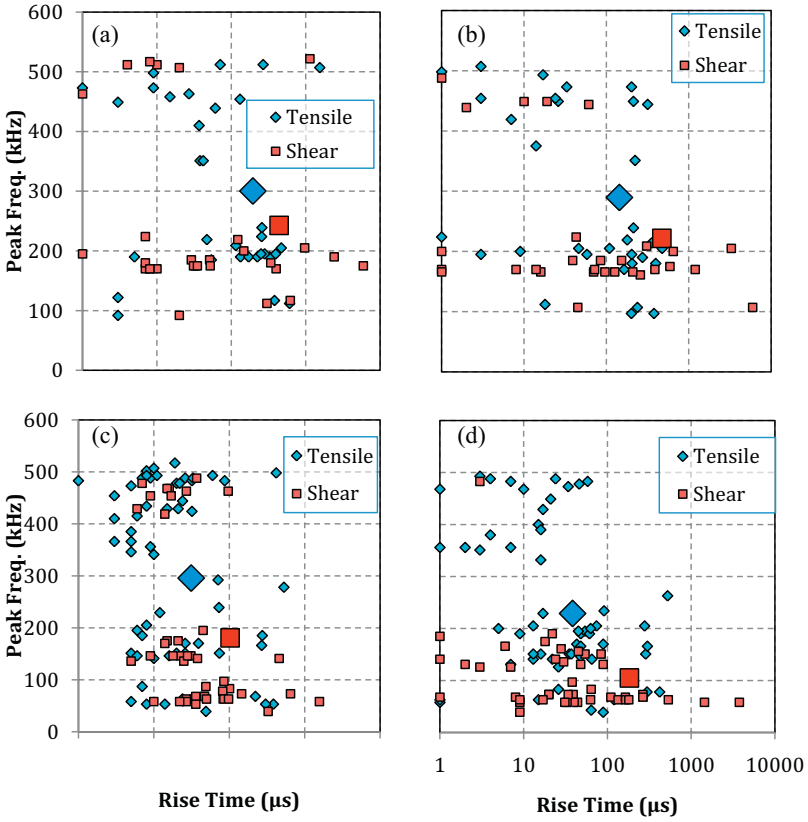

Fig. 4. Peak frequency vs. rise time for all the events recorded in marble by (a) the near sensor, (b) the furthest sensor, (c) and (d) concern events in mortar for the near and the furthest sensor, respectively. (Larger symbols of each type stand for the average of the points of the same type.)

Table 1
Average values of AE parameters.

Material		Distance from event	Rise time (μs)	Peak frequency (kHz)	Amp (dB)
Marble	Tensile	Close (15 mm)	136 (101%)	300.3 (47%)	48.1 (8%)
		Far (55 mm)	144 (71%)	289.6 (48%)	47.9 (8%)
	Shear	Close (15 mm)	439 (263%)	242.8 (56%)	52.8 (13%)
		Far (55 mm)	472 (256%)	221.7 (49%)	51.5 (13%)
Mortar	Tensile	Close (15 mm)	31.3 (191%)	295.5 (57%)	57.9 (12%)
		Far (55 mm)	38.3(135%)	229.2 (62%)	52.6 (11%)
	Shear	Close (15 mm)	102.6 (245%)	180.6 (85%)	53.5 (13%)
		Far (55 mm)	182.9 (320%)	104.9 (68%)	49.2 (13%)

Coefficients of variation is given in parenthesis.

to employ both types of materials in this study. Fig. 4c and d shows the correlation plots between PF and RT for cementitious materials as recorded by the near and the far sensor, respectively. The trends only slightly change compared to the behavior of marble. For the nearest sensor (Fig. 4c) two main groups of points are observed. The higher frequency group (400–500 kHz) is much more densely populated by events of the tensile mode than shear, while several events with peak frequencies below 200 kHz are noted for both modes. Concerning the furthest sensor in Fig. 4d, the shear mode exhibits only one event near 500 kHz while the number of tensile events remains large though certainly reduced compared to the nearest sensor. The drop of average value of PF (see large symbols, especially of the "shear" signals) between the two sensors is more evident for mortar than for marble, something attributed to the more attenuative microstructure of cementitious materials. Concerning RT the differences are similarly strong with the RT of the shear events being approximately 3 times longer than tensile in average value.

In order to discuss the trends on a firm basis, Table 1 includes the average and coefficient of variation of important AE parameters. Therefore, comparisons can be made between different materials, fracture modes and distances to the crack. The first trend that should be pointed out is that the "shear" events repeatedly exhibit longer RT than the "tensile" for the same material and sensor distance. For marble, the average RT of the tensile mode is around 140 μs while for shear it is almost 440 μs being more than three times longer. The increase is analogous for mortar with the values being in general much shorter than marble (31 μs for tension compared to 103 μs for shear). Concerning frequency characteristic, shear fracture exhibits constantly lower PF than tension (e.g. 243 kHz compared to 300 kHz for marble and 180 kHz compared to 296 kHz for mortar for the nearest sensor).

It is worth to mention that the additional propagation distance of 40 mm has a strong effect on the waveform shape. It increases RT for all materials (6–7% for marbles and up to 75% for mortar). This is related to the microstructure of the material, which exhibits stronger scattering characteristics in cement-based materials. The energy of an ultrasonic pulse propagating through the medium is dispersed in time due to multiple scattering on inhomogeneities (Tsinopoulos et al., 1999) and this has an effect on the duration of the rising part as well as the main frequency content of the signal. Similarly the PF is consistently lower at the 2nd transducer for all cases. The decrease between sensors is again more evident in mortar where PF drops by about 70 kHz, while the decrease in marble is less than or about 20 kHz. The same decreasing trend is noted for amplitude, where events in marble suffer a drop of about 1 dB, while events in mortar lose 4–5 dB for the additional propagation of 40 mm, something again attributed to the microstructure of cementitious materials.

For AE waveform features the variation is quite large and especially for the RT the coefficient of variation (standard deviation over the average) is of the order of 100% or more. This is inherent to AE measurements since the amount of crack displacement during each event and the state of the material as damage is being accumulated are continuously changing. This randomness is inevitably transferred to the AE results, in contrast to e.g. ultrasonic measurements where the excitation and the medium through which propagation occurs are usually constant. Completely separating populations of tensile and shear signals would be desirable; however, the fact that the AE parameter averages of tension and mixed mode fracture are quite far apart is of great significance for material science and engineering research, as it enables the correct characterization of shifting trends in real time. It is also very important to mention that this parameter-based approach is easy to perform and requires just a few sensors in order to monitor the process offering therefore the potential for in situ use in contrast to other laboratory oriented approaches like the moment tensor analysis that requires practically eight sensors for mode classification (Ohno and Ohtsu, 2010).

It should be noted that the specific values of AE features and frequencies certainly depend on the response characteristics of the transducers. The specific sensors, although considered broad band, still exercise certain influence on the acquired waveforms. However, since the same set of transducers is used throughout the testing series, any differences can be attributed to the fracture mode or propagation distance. It is shown therefore, that broad band AE sensors can monitor the differences of fracture modes while using other set of transducers, the discrepancies would still be monitored though most likely with different values of AE parameters. It is mentioned that the above trends concern the specific materials tested. Although the AE characteristics depend on the transient displacement of the crack sides dictated by the active fracture mode, the microstructure of the materials is also important and therefore, similarities to other type of structural materials like wood or steel should not be taken for granted.

4. Conclusions

The present paper examines the experimental evidence of the AE signature of different fracture modes in cementitious mortar and marble materials under flexural load. This subject exhibits strong interest from the engineering point of view since usually a specific sequence of failure mechanisms is followed in actual fracture. Passive monitoring can reveal the dominant fracture mode and help the estimation of the remaining life of the material. Materials with different microstructure were tested in bending and shear, namely marble as a typical homogeneous material and cement mortar as a material with microstructure on the level of millimeters. Simple alterations on the experimental set up allowed triggering different fracture modes. The results show firm evidence that actually the different fracture modes (tension and mixed mode) exhibit different AE signatures in terms of frequency and waveform shape parameters like the rise time. Shear fracture exhibits lower frequency and longer waveforms in average. Collecting an adequate population of signals may certainly help to distinguish the dominant fracture mode despite the inherent variation on the

measurements. A noteworthy detail is that the distance between the cracking source and the sensor is of primary importance, since an additional propagation of 40 mm poses substantial changes in the values of AE features for both materials. Any AE monitoring should therefore, be combined with elastic wave propagation study since the distortion and attenuation imposed by the medium may well mask the original characteristics of the emitted wave even in small laboratory samples. Future efforts should employ larger concrete specimens and recording of signal by more sensors and longer propagation distances while the testing set up could be improved by the aid of FEM analysis in order to result to pure shear fracture instead of mixed mode.

Acknowledgements

This research project has been co-financed by the European Union (European Regional Development Fund – ERDF) and Greek national funds through the Operational Program "THESSALY MAINLAND GREECE AND EPIRUS-2007-2013" of the National Strategic Reference Framework (NSRF 2007-2013).

References

Aggelis, D.G., 2011. Classification of cracking mode in concrete by acoustic emission parameters. Mechanics Research Communications 38, 153–157.

Aggelis, D.G., Barkoula, N.M., Matikas, T.E., Paipetis, A.S., 2010. Acoustic emission monitoring of degradation of cross ply laminates. Journal of the Acoustical Society of America 127 (6), EL246–EL251.

Aggelis, D.G., Kordatos, E.Z., Matikas, T.E., 2011. Acoustic emission for fatigue damage characterization in metal plates. Mechanics Research Communications 38, 106–110.

Aggelis, D.G., Mpalaskas, A.C., Ntalakas, D., Matikas, T.E., 2012. Effect of wave distortion on acoustic emission characterization of cementitious materials. Construction and Building Materials 35, 183–190.

Ohno, K., Ohtsu, M., 2010. Crack classification in concrete based on acoustic emission. Construction and Building Materials 24 (12), 2339–2346.

Ohtsu, M., 2010. Recommendations of RILEM Technical Committee 212-ACD: acoustic emission and related NDE techniques for crack detection and damage evaluation in concrete: 3. Test method for classification of active cracks in concrete structures by acoustic emission. Materials and Structures 43 (9), 1187–1189.

PAC website. http://www.mistrasgroup.com/products/solutions/acousticemission/sensors/

Sause, M.G.R., Müller, T., Horoschenkoff, A., Horn, S., 2012. Quantification of failure mechanisms in mode-I loading of fiber reinforced plastics utilizing acoustic emission analysis. Composites Science and Technology 72 (2), 167–174.

Shiotani, T., 2006. Evaluation of long-term stability for rock slope by means of acoustic emission technique. NDT&E Int 39 (3), 217–228.

Shull, P.J. (Ed.), 2002. Nondestructive evaluation, Theory, Techniques and Applications. CRC, Press, New York.

Tsinopoulos, S.V., Agnantiaris, J.P., Polyzos, D., 1999. An advanced boundary element/fast Fourier transform axisymmetric formulation for acoustic radiation and wave scattering problems. Journal of the Acoustical Society of America 105, 1517.

Van Tittelboom, K., De Belie, N., Lehmann, F., Grosse, C.U., 2012. Acoustic emission analysis for the quantification of autonomous crack healing in concrete. Construction and Building Materials 28, 333–341.

Yonezu, A., Arino, M., Kondo, T., Hirakata, H., Minoshima, K., 2010. On hydrogen induced Vickers indentation cracking in high-strength steel. Mechanics Research Communications 37, 230–234.

Zárate, B.A., Caicedo, J.M., Yu, J., Ziehl, P., 2012. Probabilistic prognosis of fatigue crack growth using acoustic emission data. Journal of Engineering Mechanics 138 (9), 1101–1111.